

Dynamics of vortex-antivortex pairs in ferromagnets

Stavros Komineas¹ and Nikos Papanicolaou²

¹*Max-Planck Institute for the Physics of Complex Systems,
Nöthnitzer Str. 38, 01187 Dresden, Germany*

²*Department of Physics, and Institute of Plasma Physics, University of Crete, Heraklion, Greece*

(Dated: June 26, 2021)

We study the dynamics of vortex-antivortex (VA) pairs in an infinitely thin ferromagnetic film with easy-plane anisotropy. These are localized excitations with finite energy that are characterized by a topological (skyrmion) number $\mathcal{N} = 0, \pm 1$. Topologically trivial ($\mathcal{N} = 0$) VA pairs undergo Kelvin motion analogous to that encountered in fluid dynamics. In contrast, topologically nontrivial ($\mathcal{N} = \pm 1$) VA pairs perform rotational motion around a fixed guiding center. We present the results of a detailed study in both cases and further demonstrate that in the presence of dissipation a rotating $\mathcal{N} = \pm 1$ VA pair shrinks to a point and is annihilated, due to the discreteness of the lattice, thus leading to a “topologically forbidden” $\Delta\mathcal{N} = 1$ process. We argue that the latter process underlies the experimentally observed vortex core switching whereby the polarity of a single vortex is reversed after collision with an $\mathcal{N} = 0$ VA pair created by a burst of an applied alternating magnetic field.

I. INTRODUCTION

The best known examples of topological magnetic solitons are magnetic bubbles or skyrmions observed in abundance in ferromagnetic films with easy-axis anisotropy [1, 2]. The experimental situation is less clear in the case of ferromagnets with easy-plane anisotropy. The relevant topological structures are theoretically predicted to be half skyrmions or vortices, with a logarithmically divergent energy that may inhibit production of an isolated vortex on an infinite film. Thus the early studies of magnetic vortex dynamics had been mostly theoretical [3, 4] drawing on various analogies with related work on ferromagnetic bubbles [5], with vortex dynamics in classical fluids and superfluids [6, 7, 8], as well as with the dynamics of interacting electric charges in a uniform magnetic field.

The situation has changed dramatically in recent years. It has been realized that a disc-shaped magnetic element, with a diameter of a few hundred of nanometers, provides an excellent geometry for the realization of a magnetic vortex configuration. In particular, the exchange energy is finite on a finite element while the magnetostatic field vanishes everywhere except at the vortex core. As a result, the vortex is actually the lowest energy magnetic state in a disc-shaped element. In other words, interest in the vortex stems from the fact that it is a nontrivial magnetic state which can, nevertheless, be spontaneously created in magnetic elements [9].

It is then natural to ask whether nontrivial magnetic states other than the single vortex may play an important role in the dynamics of magnetic elements [10, 11]. An answer to this question comes from a somewhat unlikely direction. Recent experiments have shown a peculiar dynamical behavior of vortices and magnetic domain walls when these are probed by external magnetic fields. Vortices may switch their polarity under the influence of a very weak external magnetic field of the order of a few mT [12, 13]. The same switching phenomenon was observed by passing an a.c. electrical current through a magnetic disc [14]. Since the polarity of the vortex contributes to its topological structure, the switching process clearly implies a discontinuous (topologically forbidden) change of the magnetic configuration. This is certainly a surprise especially because the external field is rather weak. The key to this phenomenon is the appearance of vortex pairs which are spontaneously created in the vicinity of existing vortices [13, 15]. The creation of topological excitations (vortex pairs) by alternating external fields had been anticipated by an early study based on collective coordinates [16].

In this paper we study vortex-antivortex pairs (VA pairs) which are nontrivial magnetic states that play an important role in the dynamics of magnetic elements. However, unlike a single vortex, a VA pair is a localized object whose energy remains finite even on an infinite film. It is then reasonable to expect that the essential features of the dynamics of VA pairs can be understood in the infinite-film approximation which is adopted in the following. A brief summary of the relevant dynamical equations and related topological structures is given in Section II. In Section III we study a VA pair in which the vortex and the antivortex carry the same polarity. Such a pair is shown to undergo translational Kelvin motion analogous to that observed in fluid dynamics [17]. In Section IV we study a VA pair in which the vortex and the antivortex carry opposite polarities. Such a pair is shown to behave as a rotating vortex dipole

[18] because its topological structure is substantially different than that of the pair in Kelvin motion.

The preceding results are combined in Section V to demonstrate that a rotating vortex dipole may be annihilated by a quasi-continuous process in spite of its nontrivial topological structure. In particular, no energy barrier has to be overcome in contrast to the usual expectations for topological solitons. This opens the possibility for switching mechanisms between topologically distinct states in ferromagnets. The possibility to change the topological structure leads to a dramatic change in the magnetization dynamics as a VA pair is created or annihilated. Such a pair annihilation process lies in the heart of the counter-intuitive vortex polarity switching event that was observed in magnetic elements [12, 13, 14].

Some concluding remarks are summarized in Section VI. Finally, an Appendix is devoted to a brief description of the dynamics of interacting electric charges in a uniform magnetic field, which also exhibits most of the peculiar features of the dynamics of VA pairs.

II. THE MODEL

A ferromagnet is characterized by the magnetization $\mathbf{m} = (m_1, m_2, m_3)$ measured in units of the constant saturation magnetization M_s . Hence \mathbf{m} is a vector field of unit length, $\mathbf{m}^2 = m_1^2 + m_2^2 + m_3^2 = 1$, but is otherwise a nontrivial function of position and time $\mathbf{m} = \mathbf{m}(\mathbf{r}, t)$ that satisfies the rationalized Landau-Lifshitz (LL) equation

$$\frac{\partial \mathbf{m}}{\partial t} = \mathbf{m} \times \mathbf{f}, \quad \mathbf{f} \equiv \Delta \mathbf{m} - q m_3 \hat{\mathbf{e}}_3, \quad \mathbf{m}^2 = 1. \quad (1)$$

Here distances are measured in units of the exchange length $\ell_{\text{ex}} = \sqrt{A/2\pi M_s^2}$, where A is the exchange constant, and the unit of time is $\tau_0 \equiv 1/(4\pi\gamma M_s)$ where γ is the gyromagnetic ratio. Typical values are $\ell_{\text{ex}} \sim 5\text{nm}$ and $\tau_0 \sim 10\text{ps}$ which set the scales for the phenomena described by Eq. (1). To complete the description of the LL equation we note that we consider ferromagnetic materials with uniaxial anisotropy. Then $\hat{\mathbf{e}}_3$ in Eq. (1) is a unit vector along the symmetry axis and the dimensionless parameter $q \equiv K/2\pi M_s^2$, where K is an anisotropy constant, measures the strength of anisotropy. In particular, q is taken to be positive throughout this paper, a choice that corresponds to easy-plane ferromagnets.

An important omission in Eq. (1) is the demagnetizing field produced by the magnetization itself [1, 2]. However, in the limit of a very thin film, the effect of the demagnetizing field is thought to amount to a simple additive renormalization of the anisotropy constant [19]. Also note that we may perform the rescalings $\sqrt{q}\mathbf{r} \rightarrow \mathbf{r}$ and $qt \rightarrow t$ which further renormalize the units of space and time discussed earlier and lead to a completely rationalized LL equation where we may set $q = 1$ without loss of generality. With this understanding, all calculations presented in this paper are based on a two-dimensional (2D) restriction of Eq. (1), i.e., $\mathbf{r} = (x, y)$ and $\Delta = \partial^2/\partial x^2 + \partial^2/\partial y^2$, while q is set equal to unity without further notice.

The effective field \mathbf{f} in Eq. (1) may be derived from a variational argument:

$$\mathbf{f} = -\frac{\delta E}{\delta \mathbf{m}}; \quad E = \frac{1}{2} \int [(\nabla \mathbf{m})^2 + m_3^2] dx dy \quad (2)$$

where E is the conserved energy functional. A standard Hamiltonian form is obtained by resolving the constraint $\mathbf{m}^2 = 1$ through, say, the spherical parameterization

$$m_1 + i m_2 = \sin \Theta e^{i\Phi}, \quad m_3 = \cos \Theta. \quad (3)$$

The LL equation is then written as

$$\frac{\partial \Phi}{\partial t} = \frac{\delta E}{\delta \Pi}, \quad \frac{\partial \Pi}{\partial t} = -\frac{\delta E}{\delta \Phi} \quad (4)$$

where $\Pi \equiv \cos \Theta$ is the canonical momentum conjugate to the azimuthal angle Φ . Taking into account the specific form of the energy in Eq. (2) or

$$E = \frac{1}{2} \int [(\nabla \Theta)^2 + \sin^2 \Theta (\nabla \Phi)^2 + \cos^2 \Theta] dx dy \quad (5)$$

the Hamilton equations (3) yield

$$\begin{aligned}\sin \Theta \frac{\partial \Phi}{\partial t} &= \Delta \Theta + [1 - (\nabla \Phi)^2] \cos \Theta \sin \Theta, \\ \sin \Theta \frac{\partial \Theta}{\partial t} &= -\nabla \cdot (\sin^2 \Theta \nabla \Phi).\end{aligned}\quad (6)$$

Another useful parameterization is obtained through the stereographic variable Ω :

$$\Omega = \frac{m_1 + i m_2}{1 + m_3}; \quad m_1 + i m_2 = \frac{2\Omega}{1 + \overline{\Omega}\Omega}, \quad m_3 = \frac{1 - \overline{\Omega}\Omega}{1 + \overline{\Omega}\Omega} \quad (7)$$

in terms of which the LL equation reads

$$i \frac{\partial \Omega}{\partial t} + \Delta \Omega + \frac{1 - \overline{\Omega}\Omega}{1 + \overline{\Omega}\Omega} \Omega = \frac{2\overline{\Omega}}{1 + \overline{\Omega}\Omega} (\nabla \Omega \cdot \nabla \Omega) \quad (8)$$

where $\overline{\Omega}$ is the complex conjugate of Ω . Equations (1),(6), and (8) are three equivalent versions of the LL equation and may be used at convenience depending on the specific calculation considered.

A key quantity for describing both topological and dynamical properties of the 2D LL equation is the local topological vorticity $\gamma = \gamma(x, y, t)$ defined from [20, 21]:

$$\gamma = \epsilon_{\alpha\beta} \partial_\alpha \Pi \partial_\beta \Phi = \epsilon_{\alpha\beta} \sin \Theta \partial_\beta \Theta \partial_\alpha \Phi = \frac{1}{2} \epsilon_{\alpha\beta} (\partial_\beta \mathbf{m} \times \partial_\alpha \mathbf{m}) \cdot \mathbf{m}, \quad (9)$$

where the usual summation convention is invoked for the repeated indices α and β , which take over two distinct values corresponding to the two spatial coordinates x and y , and $\epsilon_{\alpha\beta}$ is the 2D antisymmetric tensor. In particular, one may consider the total topological vorticity Γ and the Pontryagin index or skyrmion number \mathcal{N} defined from

$$\Gamma = \int \gamma \, dx dy, \quad \mathcal{N} = \frac{\Gamma}{4\pi}. \quad (10)$$

A naive partial integration using Eq. (9) yields $\Gamma = 0 = \mathcal{N}$ for all magnetic configurations for which such an integration is permissible. However, nonvanishing values for Γ and \mathcal{N} are possible and are topologically quantized. Specifically, for field configurations that approach a constant (uniform) magnetization at spatial infinity, the skyrmion number \mathcal{N} is quantized according to $\mathcal{N} = 0, \pm 1, \pm 2, \dots$. Half integer values are also possible in the case of field configurations with more complicated structure at infinity such as half skyrmions or vortices (see below).

The local topological vorticity γ is also important for an unambiguous definition of conservation laws in the LL equation. Hence the linear momentum (impulse) $\mathbf{P} = (P_x, P_y)$ is defined from

$$P_x = - \int y \gamma \, dx dy, \quad P_y = \int x \gamma \, dx dy, \quad (11)$$

while the angular momentum (impulse) is given by

$$L = \frac{1}{2} \int \rho^2 \gamma \, dx dy \quad (12)$$

where $\rho^2 = x^2 + y^2$. Since detailed discussions of these conservation laws have already appeared in the literature [17, 20, 21] we simply note here that analogous conservation laws were defined as moments of ordinary vorticity in fluid dynamics [6, 7].

We first search for static (time independent) solutions of the LL equation which may be obtained by omitting time derivatives in Eq. (6) and further introducing the axially symmetric ansatz $\Theta = \theta(\rho)$ and $\Phi = \kappa(\phi - \phi_0)$, where ρ and ϕ are the usual cylindrical coordinates ($x = \rho \cos \phi$, $y = \rho \sin \phi$), $\kappa = \pm 1$ will be referred to as the vortex number, and ϕ_0 is an arbitrary constant phase reflecting the azimuthal invariance. The resulting ordinary differential equation for the amplitude $\theta = \theta(\rho)$ is solved numerically with standard boundary condition $\theta(\rho \rightarrow \infty) = \pi/2$ and the result is shown in Fig. 1. The corresponding magnetization is then given by

$$m_1 + i m_2 = \sin \theta e^{i\kappa(\phi - \phi_0)}, \quad m_3 = \lambda \cos \theta, \quad (13)$$

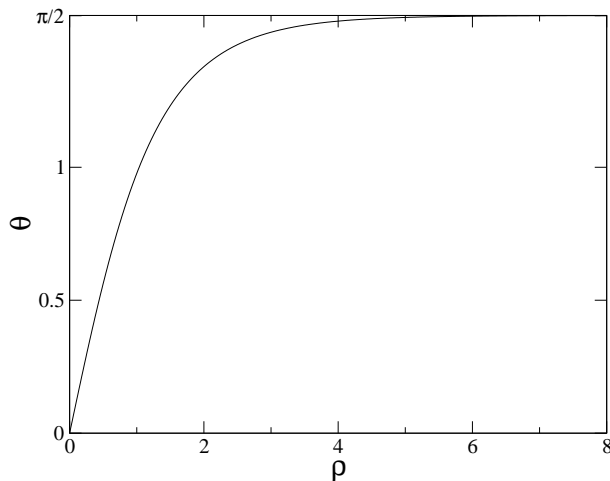


FIG. 1: Profile of a single vortex calculated numerically. The complete solution is given by Eq. (13).

where $\lambda = \pm 1$ will be called the polarity. The total energy is accordingly reduced to

$$E = \frac{1}{2} \int_0^{\infty} \left[\left(\frac{\partial \theta}{\partial \rho} \right)^2 + \frac{\sin^2 \theta}{\rho^2} + \cos^2 \theta \right] (2\pi \rho d\rho). \quad (14)$$

where the centrifugal (second) term is logarithmically divergent for the assumed boundary condition at spatial infinity. However, the anisotropy energy given by the last term is finite and is actually predicted to be

$$E_a = \frac{1}{2} \int_0^{\infty} \cos^2 \theta (2\pi \rho d\rho) = \frac{\pi}{2} \quad (15)$$

by a careful derivation of a suitable virial relation [22]. Finally, the total vorticity Γ and the skyrmion number \mathcal{N} are calculated from Eq. (10) to be

$$\Gamma = -2\pi\kappa\lambda, \quad \mathcal{N} = -\frac{1}{2}\kappa\lambda, \quad (16)$$

where the vortex number $\kappa = \pm 1$ and the polarity $\lambda = \pm 1$ may be taken in any combination. Thus, we must consider four possibilities; namely, a vortex that comes in two varieties ($\kappa = 1, \lambda = \pm 1$) and thus $\mathcal{N} = \mp 1/2$, and an antivortex which also comes in two varieties ($\kappa = -1, \lambda = \pm 1$) and thus $\mathcal{N} = \pm 1/2$. In all cases the calculated static solution is a topological soliton with half integer skyrmion number, in contrast to ordinary skyrmions (such as magnetic bubbles) which carry integer \mathcal{N} .

Our main aim in the continuation of this paper is to search for nontrivial solutions that may combine a vortex and an antivortex (VA pair) in a way that the total energy is finite. We leave aside for the moment the LL equation and construct model VA pairs in terms of the basic single-vortex configuration described above. This is easily accomplished by invoking the stereographic variable Ω of Eq. (7) to write a single (κ, λ) vortex located at the origin of coordinates as

$$\Omega = \frac{\sin \theta}{1 + \lambda \cos \theta} e^{i\kappa(\phi - \phi_0)} \quad (17)$$

where $\theta = \theta(\rho)$ is the vortex profile taken from Fig. 1 or simply the model profile defined from $\cos \theta = 1/\cosh \rho$ and $\sin \theta = \tanh \rho$. We now produce two replicas of the basic vortex to describe a pair of vortices by the product ansatz

$$\Omega = \Omega_1 \Omega_2 \quad (18)$$

where Ω_1 is configuration (17) applied for $(\kappa, \lambda) = (\kappa_1, \lambda_1)$ and the origin displaced to, say, $(x, y) = (-d/2, 0)$ while Ω_2 is a (κ_2, λ_2) vortex located around $(x, y) = (d/2, 0)$. The skyrmion number of this

configuration is given by

$$\mathcal{N} = -\frac{1}{2}(\kappa_1\lambda_1 + \kappa_2\lambda_2) \quad (19)$$

and its energy is finite only if we restrict attention to vortex-antivortex (VA) pairs ($\kappa_1 = -\kappa_2$). For definiteness we choose $\kappa_1 = 1$ and $\kappa_2 = -1$ and thus the skyrmion number

$$\mathcal{N} = -\frac{1}{2}(\lambda_1 - \lambda_2) \quad (20)$$

depends on the polarities λ_1 and λ_2 . Now a VA pair with equal polarities ($\lambda_1 = \lambda_2 = \pm 1$) is topologically trivial ($\mathcal{N} = 0$). In contrast, a VA pair with opposite polarities is topologically equivalent to a skyrmion ($\mathcal{N} = 1$, for $\lambda_1 = -1$ and $\lambda_2 = 1$) or an antiskyrmion ($\mathcal{N} = -1$, for $\lambda_1 = 1$ and $\lambda_2 = -1$). In all three cases configuration (18) carries finite energy because its overall phase cancels out at spatial infinity where the magnetization approaches the uniform configuration $\mathbf{m} = (1, 0, 0)$ modulo an overall azimuthal rotation which depends on the choice of individual phases ϕ_0 in the ansatz (18). This explains, in particular, why VA pairs are characterized by an integer skyrmion number ($\mathcal{N} = 0, \pm 1$).

Needless to say, the VA pairs constructed above are not solutions of the LL equation. Yet an interesting picture arises when configuration (18) is used as an initial condition in the complete equation (8). A topologically trivial ($\mathcal{N} = 0$) VA pair undergoes Kelvin motion in which the vortex and the antivortex initially located at a relative distance d along the x axis move in parallel along the y axis with nearly constant velocity. In contrast, a topologically nontrivial ($\mathcal{N} = \pm 1$) VA pair undergoes rotational motion around a fixed guiding center at nearly constant angular velocity. In both cases the main trajectories are decorated by Larmor-type oscillations [23] which are tamed when the relative distance between the vortex and the antivortex is large. The effect of the polarity of vortex pairs has been studied experimentally in patterned ferromagnetic ellipses [24]. Two vortices were created an ellipse and it was found that their dynamics depended on their relative polarity, as is indicated by Eq. (20).

In the following two sections we examine the two cases in turn. In particular, we aim at constructing true steady-state solitary waves that describe VA pairs in pure Kelvin motion for $\mathcal{N} = 0$ and pure rotational motion for $\mathcal{N} = \pm 1$.

III. KELVIN MOTION

As the title of this section suggests, VA pairs in Kelvin motion were originally studied in the context of ordinary fluid dynamics [6, 7]. A further analogy exists with the 2D motion of an electron-positron pair interacting via the Coulomb potential and placed in a uniform magnetic field perpendicular to the plane. If the electron and the positron are initially at rest their guiding centers will move along two parallel straight lines while the actual trajectories will display the familiar Larmor oscillations. However, when the electron and the positron are given a common initial velocity such that the Coulomb force is exactly balanced by the magnetic force, both the guiding centers and the actual positions of the charges will move steadily along parallel lines, even though the two sets of trajectories do not coincide. The resulting special configuration may be thought of as a peculiar electron-positron bound state in steady translational motion (see our Appendix).

It is thus reasonable to expect that a solitary wave exists in a 2D easy-plane ferromagnet which describes a VA pair that proceeds rigidly (without Larmor oscillations) in a direction perpendicular to the line connecting the vortex and the antivortex, probably because the mutual force is exactly balanced by a topological ‘‘Magnus force’’. The actual existence of such a solitary wave was established in Ref. [17] whose main result is briefly reviewed in the remainder of this section.

As it turns out, when the relative distance is large, the sought after solitary wave resembles in its gross features the model VA pair of Eq. (18) applied for, say, $\kappa_1 = -\kappa_2 = 1$ and $\lambda_1 = \lambda_2 = 1$ (thus $\mathcal{N} = 0$). We may then invoke this model to motivate some important asymptotic results valid for large d . For instance, the local topological vorticity γ is then peaked around the two points $(x, y) = (-d/2, 0)$ and $(x, y) = (d/2, 0)$ with weights -2π and 2π respectively, corresponding to the total vorticities Γ of the individual vortex and antivortex. Then the impulse defined from Eq. (11) yields $P_x = 0$, thanks to reflexion symmetry, while $P = P_y \sim 2\pi d$. One may also invoke the Derrick-like scaling relation applied to the extended energy functional $F = E - vP$:

$$vP = \int m_3^2 dx dy = 2E_a \quad (21)$$

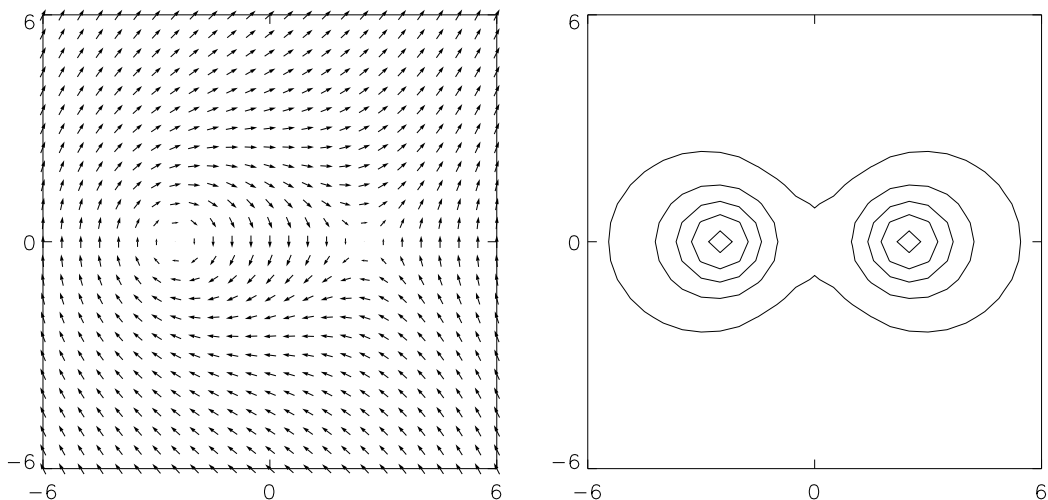


FIG. 2: Snapshot of a topologically trivial ($\mathcal{N} = 0$) VA pair in Kelvin motion, illustrated through the (m_1, m_2) projection of the magnetization $\mathbf{m} = (m_1, m_2, m_3)$ on the plane of the film (left panel) as well as level contours of m_3 (right panel). The contour levels $m_3 = 0.1, 0.3, 0.5, 0.7, 0.9$ are shown. The outer curve corresponds to $m_3 = 0.1$, while the two smallest circles are the contours for $m_3 = 0.9$ and surround the two vortex centers. The pair moves along the y axis with velocity $v = 0.2$ at a calculated relative distance $d = 4.97$ (along the x axis), energy $E = 20$, and impulse $P = 30$.

where E_a is the total anisotropy energy of the VA pair. For large d this energy approaches the sum of the anisotropy energies of the individual vortex and antivortex, each given by $\pi/2$ in view of the virial relation (15). Hence, $\int m_3^2 dx dy \sim 2(\pi/2 + \pi/2) = 2\pi$ and $vP \sim 2\pi$. To summarize,

$$P \sim 2\pi d, \quad vP \sim 2\pi, \quad v \sim \frac{1}{d}. \quad (22)$$

One may further consider the familiar group-velocity relation

$$v = \frac{dE}{dP} \quad (23)$$

in which we insert the estimate $v \sim 2\pi/P$ to obtain an elementary differential equation for E whose integral is

$$E \approx 2\pi \ln(P/P_0) \quad (24)$$

where P_0 is an integration constant that cannot be fixed by the present leading-order argument. Nevertheless, Eq. (24) provides the essence of the energy-momentum dispersion at large relative distance d or small velocity $v \sim 1/d$ and hence large momentum $P \sim 2\pi d$.

To obtain an accurate numerical solution it is convenient to work with the stereographic variable Ω of Eq. (7). Then the LL Eq. (8) restricted to a solitary wave in rigid motion with constant velocity v along, say, the y axis reads

$$-iv \frac{\partial \Omega}{\partial y} + \Delta \Omega + \frac{1 - \bar{\Omega} \Omega}{1 + \bar{\Omega} \Omega} \Omega = \frac{2\bar{\Omega}}{1 + \bar{\Omega} \Omega} (\nabla \Omega \cdot \nabla \Omega) \quad (25)$$

and is supplemented by the boundary condition $\Omega \rightarrow 1$ at spatial infinity where the magnetization approaches a uniform configuration. Once a solution $\Omega = \Omega(x, y; v)$ of Eq. (25) is obtained for a specific value of the velocity v , the sought after solitary wave is given by $\Omega(x, y - vt; v)$.

Equation (25) was solved numerically via a Newton-Raphson iterative algorithm for velocities in the range $0.1 \leq v < 0.99$. Note that $v = 1$ is the familiar magnon velocity (in rationalized units) and provides an upper bound for the existence of a solitary wave in rigid motion. On the contrary, there is no lower bound for the velocity – the restriction $v \geq 0.1$ was dictated only by numerical expedience. Now, the calculated solitary wave is illustrated in Fig. 2 for the relatively low velocity $v = 0.2$ and does indeed

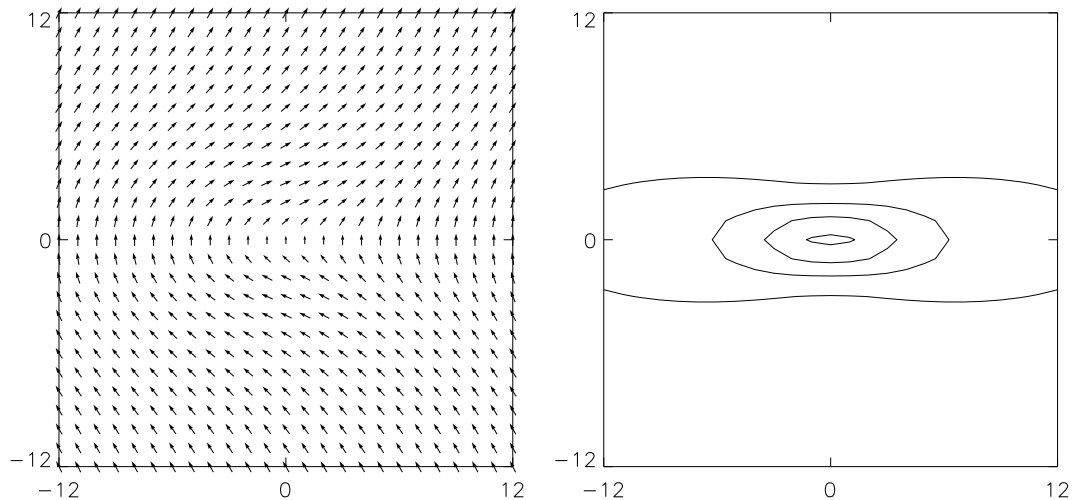


FIG. 3: Solitary wave in Kelvin motion with $v = 0.95$ along the y axis (conventions as in Fig. 2). Note that the vortex-antivortex character is lost ($d = 0$) and the wave is a lump with no apparent topological features. The calculated energy and impulse are $E = 18$ and $P = 17$.

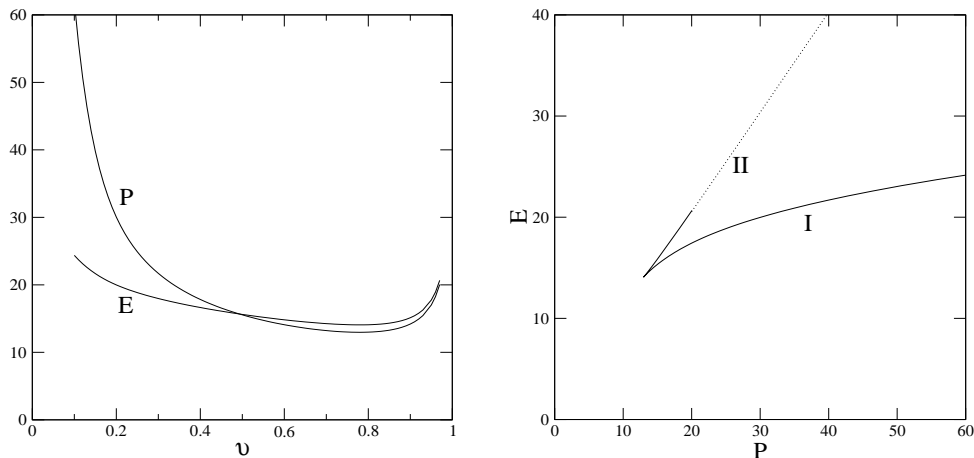


FIG. 4: Energy E and impulse P as functions of velocity v (left panel) and E vs P dispersion (right panel) for a solitary wave in Kelvin motion. The dotted line was calculated from the asymptotic dispersion (26) applied for $Q_0 = 4.7$.

describe a VA pair (with $\mathcal{N} = 0$) at a relative distance $d = 4.97 \sim 1/v$, as anticipated by the discussion of model VA pairs in Section II and the heuristic asymptotic analysis earlier in this section. But we are now in a position to carry out an accurate calculation practically throughout the allowed range $0 < v < 1$, to discover that there exists a characteristic velocity $v_0 \sim 0.78$ above which the vortex-antivortex character is lost ($d \sim 0$) and the solitary wave becomes a lump with no apparent topological features, as illustrated in Fig. 3 for $v = 0.95$.

The existence of a characteristic velocity v_0 becomes apparent when we calculate energy E and impulse P as functions of v , as shown in Fig. 4. Note that both E and P develop a minimum at a common velocity $v = v_0 = 0.78$. As a result, the energy vs impulse dispersion shown in Fig. 4 develops a cusp at a point (E_0, P_0) that corresponds to the values of E and P at $v = v_0$. Thus the calculated family of solitary waves consists of two branches. Branch I consists of VA pairs that propagate with velocities in the range $v < v_0$. The corresponding branch in the dispersion of Fig. 4 approaches the asymptotic dispersion (24) for large P (or $v \rightarrow 0$). Indeed, an excellent fit of the data is obtained by Eq. (24) if we choose the subleading constant according to $\ln P_0 \sim 1/4$. Branch II consists of lumps with no apparent topological features which propagate with velocities in the range $v_0 < v < 1$. The corresponding branch in the dispersion of

Fig. 4 is accurately described in the asymptotic ($v \rightarrow 1$) region, where P again becomes large, by

$$E = P \left(1 + \frac{Q_0^2}{2P^2} + \dots \right) \quad (26)$$

with $Q_0 \approx 4.7$. Actually this asymptotic dispersion can be derived by showing that in the limit $v \rightarrow 1$ the 2D Landau-Lifshitz equation reduces to what is a modified Kadomtsev-Petviashvili (KP) equation [17].

A cusp in the energy vs impulse dispersion occurred previously in a calculation of vortex rings in a model superfluid by Jones and Roberts [25]. The same authors together with Putterman later argued that the solitary waves that correspond to branch II are actually unstable [26]. Interestingly, a dispersion with a cusp appears also in the much simpler problem of electron-positron motion in a uniform magnetic field, where the motion that corresponds to branch II is also unstable (see our Appendix). Hence, while a stability analysis has not yet been carried out for the solitary waves described in this section, it is reasonable to expect that the lumps of branch II may be unstable. But there is every reason to believe that the Kelvin motion of the VA pairs of branch I is indeed stable.

IV. ROTATIONAL MOTION

The possibility of topologically nontrivial ($\mathcal{N} = \pm 1$) VA pairs in steady rotational motion was recently examined by one of us [18]. Again, one may invoke the model VA pair of Section II to understand some important features of the rotational motion at large distance d . For definiteness we consider a VA pair defined by Eq. (18) with $\kappa_1 = -\kappa_2 = 1$ and $\lambda_1 = -\lambda_2 = -1$, thus $\mathcal{N} = 1$. The local topological vorticity γ is then peaked around the positions of the vortex and the antivortex, now with weight equal to 2π in both cases. Then, for large d , the angular momentum defined by Eq. (12) is estimated to be $L \sim \frac{1}{2}2(2\pi)(\frac{d}{2})^2 = \frac{\pi}{2}d^2$. One may also consider the Derrick-like scaling relation applied to the extended energy functional $F = E - \omega L$:

$$\omega L = \frac{1}{2} \int m_3^2 dx dy = E_a \quad (27)$$

where E_a is the total anisotropy energy of a VA pair which approaches asymptotically $E_a \sim (\frac{\pi}{2} + \frac{\pi}{2}) = \pi$, and hence $\omega L = \pi$, because the anisotropy energy of a single vortex is equal to $\pi/2$ according to Eq. (15). To summarize,

$$L \sim \frac{\pi}{2} d^2, \quad \omega L \sim \pi, \quad \omega \sim \frac{2}{d^2}. \quad (28)$$

One may further employ the familiar relation

$$\omega = \frac{dE}{dL} \quad (29)$$

in which we insert the estimate $\omega \sim \pi/L$ to obtain an elementary differential equation for E whose integral is

$$E \approx \pi \ln(L/L_0) \quad (30)$$

where L_0 is an integration constant that cannot be fixed by the present leading-order argument. Nevertheless, Eq. (30) provides the essence of the energy vs angular momentum dispersion for large relative distance d or small angular frequency $\omega \sim 2/d^2$ and hence large angular momentum $L \sim \frac{\pi}{2} d^2$.

While the preceding heuristic asymptotic analysis is very useful for understanding some basic aspects of a rotating VA pair, it does not give us any clue concerning the fate of the pair at small vortex-antivortex separation. In principle, such a question could be settled by solving numerically the analog of Eq. (25) for a solitary wave rotating at constant angular frequency ω :

$$i\omega \epsilon_{\alpha\beta} x_\alpha \partial_\beta \Omega + \Delta \Omega + \frac{1 - \overline{\Omega}}{1 + \overline{\Omega}} \Omega = \frac{2\overline{\Omega}}{1 + \overline{\Omega}} (\nabla \Omega \cdot \nabla \Omega). \quad (31)$$

A numerical solution could again be attempted by an iterative Newton-Raphson algorithm. Actually, in this case, we found it more convenient to employ a relaxation algorithm to derive approximate numerical solutions as stationary points of the extended energy functional $F = E - \omega L$ [18].

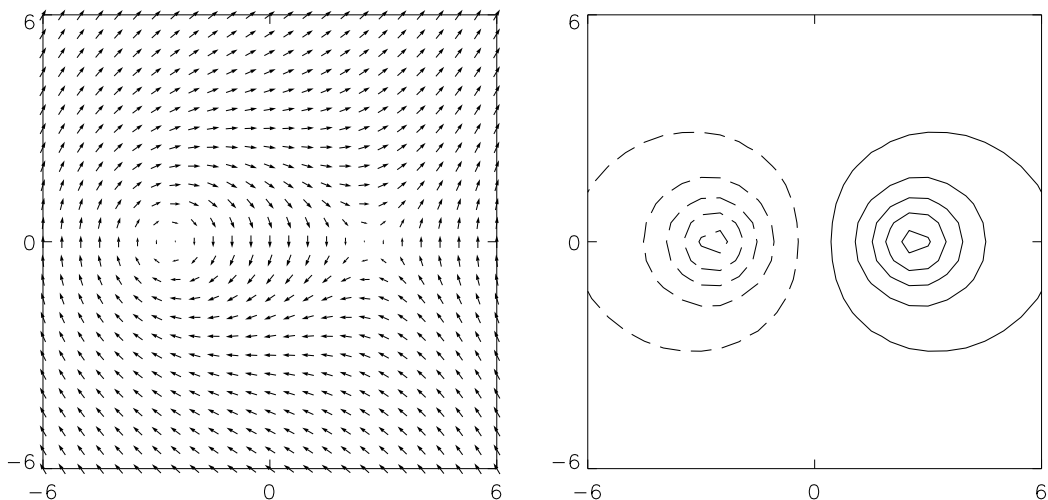


FIG. 5: Snapshot of a topologically nontrivial ($\mathcal{N} = 1$) VA pair in rotational motion (conventions as in Fig. 2, with solid lines in the right panel corresponding to positive values of m_3 and dashed lines to negative ones). The pair rotates around a fixed guiding center taken at the origin of coordinates, with angular velocity $\omega = 0.06$ and calculated relative distance $d = 5.3$, energy $E = 21$, and angular impulse $L = 64$.

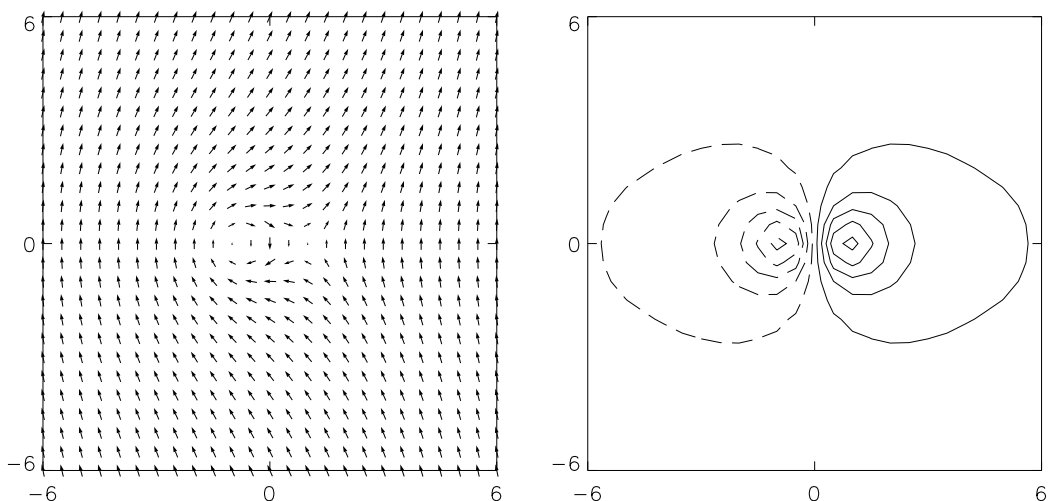


FIG. 6: $\mathcal{N} = 1$ VA pair in rotational motion with angular velocity $\omega = 0.18$ and calculated relative distance $d = 1.7$, energy $E = 15$, and angular impulse $L = 11$. The only difference from Fig. 5 is that the overall size of the pair is now reduced.

The calculated configuration for $\omega = 0.06$ is shown in Fig. 5 and does indeed correspond to a topologically nontrivial ($\mathcal{N} = 1$) rotating VA pair consisting of a vortex with negative polarity $(\kappa, \lambda) = (1, -1)$ and an antivortex with positive polarity $(\kappa, \lambda) = (-1, 1)$, as anticipated by the general discussion of Section II. In particular, for this relatively small value of ω , the calculated distance d in the rotating pair is relatively large ($d = 5.3$), so is the angular momentum ($L = 64$); in rough agreement with the asymptotic estimates of Eq. (28).

The calculation was repeated for a larger value of angular velocity ($\omega = 0.18$) to find that both the relative distance ($d = 1.7$) and the angular momentum ($L = 11$) are reduced to smaller values. But the general structure of the solution shown in Fig. 6 for $\omega = 0.18$ remains basically the same as that for $\omega = 0.06$, except that the overall size of the VA pair is reduced. For yet larger values of ω the angular momentum L tends to vanish. This trend is apparent in Fig. 7 which illustrates the dependence of E and angular momentum L as functions of angular velocity ω , as well as the E vs L dispersion. For large values of L the above dispersion exhibits logarithmic dependence, as predicted by the asymptotic result

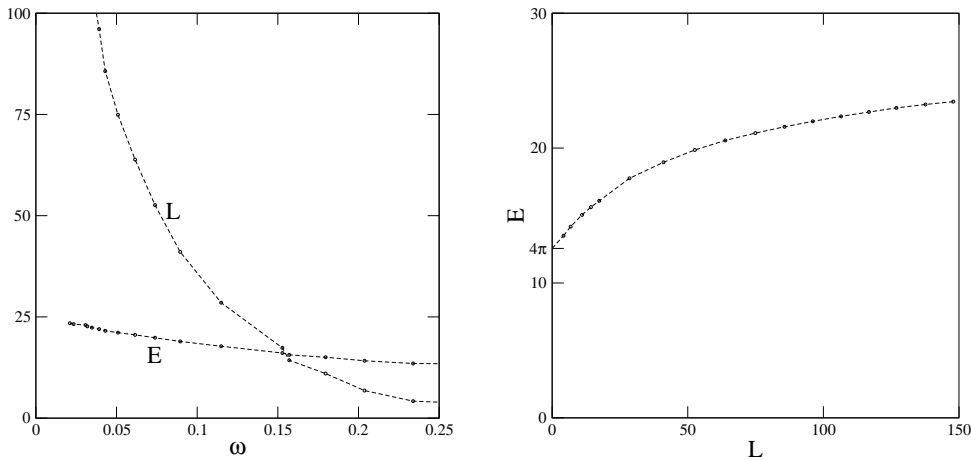


FIG. 7: Energy E and angular impulse L as functions of angular velocity ω (left panel) and E vs L dispersion (right panel) for an $\mathcal{N} = 1$ VA pair in rotational motion.

of Eq. (30). But the most important feature of the calculated dispersion is that energy approaches the finite value $E = 4\pi$ as $L \rightarrow 0$, while the corresponding rotating VA pair becomes vanishingly small. This result is of central importance for our main argument and will be analyzed in some detail in the remainder of this section.

The best way to describe a vanishing VA pair, in the limit $L \rightarrow 0$, is to invoke yet another model configuration through the stereographic variable

$$\Omega = \frac{\bar{\zeta} - \frac{d}{2}}{\zeta + \frac{d}{2}}, \quad \zeta = x + iy, \quad \bar{\zeta} = x - iy, \quad (32)$$

where the constant d is taken to be real for simplicity. Now, configuration (32) reaches a finite value $\Omega = 1$ at spatial infinity and the corresponding magnetization is uniform:

$$\mathbf{m} = (1, 0, 0) \quad \text{as} \quad |\zeta| \rightarrow \infty \quad (33)$$

which is an appropriate boundary value (modulo a constant azimuthal rotation) for easy-plane anisotropy discussed here. Because of (33) the skyrmion number is expected to be an integer and is actually computed to be $\mathcal{N} = 1$ by a direct application of Eq. (10). Furthermore, the spin configuration derived from (32) is an exact solution of the LL equation, if we neglect anisotropy, with exchange energy

$$E = E_e = \frac{1}{2} \int (\nabla \mathbf{m} \cdot \nabla \mathbf{m}) \, dx dy = 4\pi, \quad (34)$$

for any d , as discussed long time ago by Belavin and Polyakov [27].

We now return to the main line of argument by noting that configuration (32) may also be thought of as a topologically nontrivial ($\mathcal{N} = 1$) model VA pair consisting of a $(\kappa, \lambda) = (1, -1)$ vortex and a $(\kappa, \lambda) = (-1, 1)$ antivortex located at a distance d apart, in close analogy with the model VA pair constructed in Section II. Although (32) is not an exact solution in the presence of anisotropy, it provides a good model for the behavior of a vanishing VA pair in the limit $L \rightarrow 0$. Anisotropy sets a distance scale $R \sim 1/\sqrt{q} = 1$ (in rationalized units) beyond which a physically acceptable configuration must reach the uniform value (33). In a sense, this property is shared by configuration (32) because it becomes uniform almost everywhere when $d \ll 1$ while it retains its topological structure as long as d remains finite. The strict limit $d \rightarrow 0$ is not uniform. If taken naively, all topological structure appears to be lost and both energy E and skyrmion number \mathcal{N} appear to vanish. However, if integrals are performed before taking the $d \rightarrow 0$ limit, E approaches 4π without encountering an energy barrier while $\mathcal{N} = 1$ for all d . Clearly the limit $d \rightarrow 0$ creates a singular point which hides all topological structure. The main point is the claim that a similar situation arises in the calculated rotating VA pair in the limit $L \rightarrow 0$, as discussed further in Section V.

This section is completed with a comment concerning the manner in which the $L \rightarrow 0$ limit is reached. Our numerical data as well as virial relation (27) are consistent with a linear dispersion

$$E \approx 4\pi + \frac{1}{2} L \quad (35)$$

in the limit $L \rightarrow 0$, which implies a finite value of the angular velocity $\omega = dE/dL = 1/2$ in the limit of a vanishing VA pair, and thus an upper limit $\omega_{\max} \approx 1/2$.

V. VORTEX CORE SWITCHING

Applied for long time intervals, our relaxation algorithm revealed some tendency for instability of a rotating VA pair, probably due to radiation effects analogous to those expected for a pair of rotating electric charges discussed in the Appendix. However, the basic features of rotating VA pairs studied in the preceding section persist over sufficiently long time intervals and are thus relevant for practical applications. In fact, in a realistic ferromagnet, some dissipation is always present and can be modeled by introducing Gilbert damping in the LL equation through the replacement

$$\frac{\partial \mathbf{m}}{\partial t} \rightarrow \frac{\partial \mathbf{m}}{\partial t} + \alpha \left(\mathbf{m} \times \frac{\partial \mathbf{m}}{\partial t} \right) \quad \text{or} \quad i \frac{\partial \Omega}{\partial t} \rightarrow (i - \alpha) \frac{\partial \Omega}{\partial t} \quad (36)$$

in Eq. (1) or Eq. (8), respectively, where α is a dissipation constant.

The dynamics of a topologically nontrivial ($\mathcal{N} = \pm 1$) VA pair may thus be summarized as follows. The vortex and the antivortex rotate around each other, while the pair shrinks due to dissipation. The energy of the pair follows approximately the curve of the right panel of Fig. 7 as its size (and its angular momentum) decreases. At vanishing size a singular point of the type discussed in the preceding section would be created and the total energy would reach the finite value $E = 4\pi$ (in rationalized units). However, the discreteness of the lattice actually interrupts the process when the size of the pair becomes comparable to the lattice spacing. The VA pair disappears (i.e., the skyrmion number changes abruptly from $\mathcal{N} = \pm 1$ to $\mathcal{N} = 0$) and a burst of energy equal to 4π is released into the system, probably in the form of spin waves. In physical units, the amount of energy released is given by $E = 8\pi tA$ where t is the film thickness and A the exchange constant. For typical values $t = 10$ nm and $A = 10^{-11}$ J/m we obtain the estimate $E \sim 2.5 \times 10^{-18}$ J which is apparently in rough agreement with numerical simulations [28, 29].

The scenario described above explains how a topologically forbidden ($\Delta\mathcal{N} = 1$) transition can take place in a real ferromagnet but does not by itself account for the experimentally observed vortex core switching. The complete scenario involves two distinct steps. First, application of a short burst of an alternating magnetic field creates a VA pair in the vicinity of a preexisting single vortex. Second, a three-body collision takes place during which a suitable pair of vortices is annihilated through a $\Delta\mathcal{N} = 1$ transition of the type described above, and the final product is a single vortex with polarity opposite to that of the original vortex [13]. We also note that a system with three vortices (two vortices and an antivortex which form a cross-tie wall) was observed in a rectangular platelet in [30]. Their spectrum of eigenmodes was studied experimentally.

Here we do not address the question of how a VA pair is actually created. Rather we concentrate on step 2 of the process and explain in some detail how vortex core switching may occur in a three-body collision. Specifically, let us assume that a single $(1, -1)=C$ vortex is initially at rest at some specified point which is taken to be the origin of the coordinate system. Let us further assume that a topologically trivial ($\mathcal{N} = 0$) VA pair consisting of a $(1, 1)=A$ vortex and a $(-1, 1)=B$ antivortex is somehow created in the neighborhood of the original vortex. Once created the AB pair will undergo Kelvin motion of the type described in Section III and eventually collide with the single vortex C.

The process was simulated by a numerical solution of the corresponding initial-value problem in the LL equation. Figure 8 provides an illustration with three characteristic snapshots in the case of a relatively slow Kelvin pair initially moving along the y axis with velocity $v = 0.1$ for which the vortex and the antivortex are separated by a distance $d \approx 1/v = 10$. As the pair approaches, the original $C=(1, -1)$ vortex teams up with the $B=(-1, 1)$ partner of the AB pair to form a new, topologically nontrivial ($\mathcal{N} = 1$) VA pair in quasi-rotational motion. In fact, B rotates almost a full circle around C before rejoining its original partner A. The new AB pair is again a topologically trivial ($\mathcal{N} = 0$) VA pair in Kelvin motion that moves away from the target vortex, having suffered a total scattering angle that is greater than $\pi/2$ from its original direction. The scattering is inelastic in the sense that the outgoing AB pair moves out with greater velocity ($v = 0.15$). And, most remarkably, the target vortex C moves away from the origin and comes to rest at a new location in the fourth quadrant of the xy plane.

This rather unusual behavior is explained by the unusual nature of the conservation laws (11) and (12) which allow for a transmutation between position and impulse in the case of topologically nontrivial

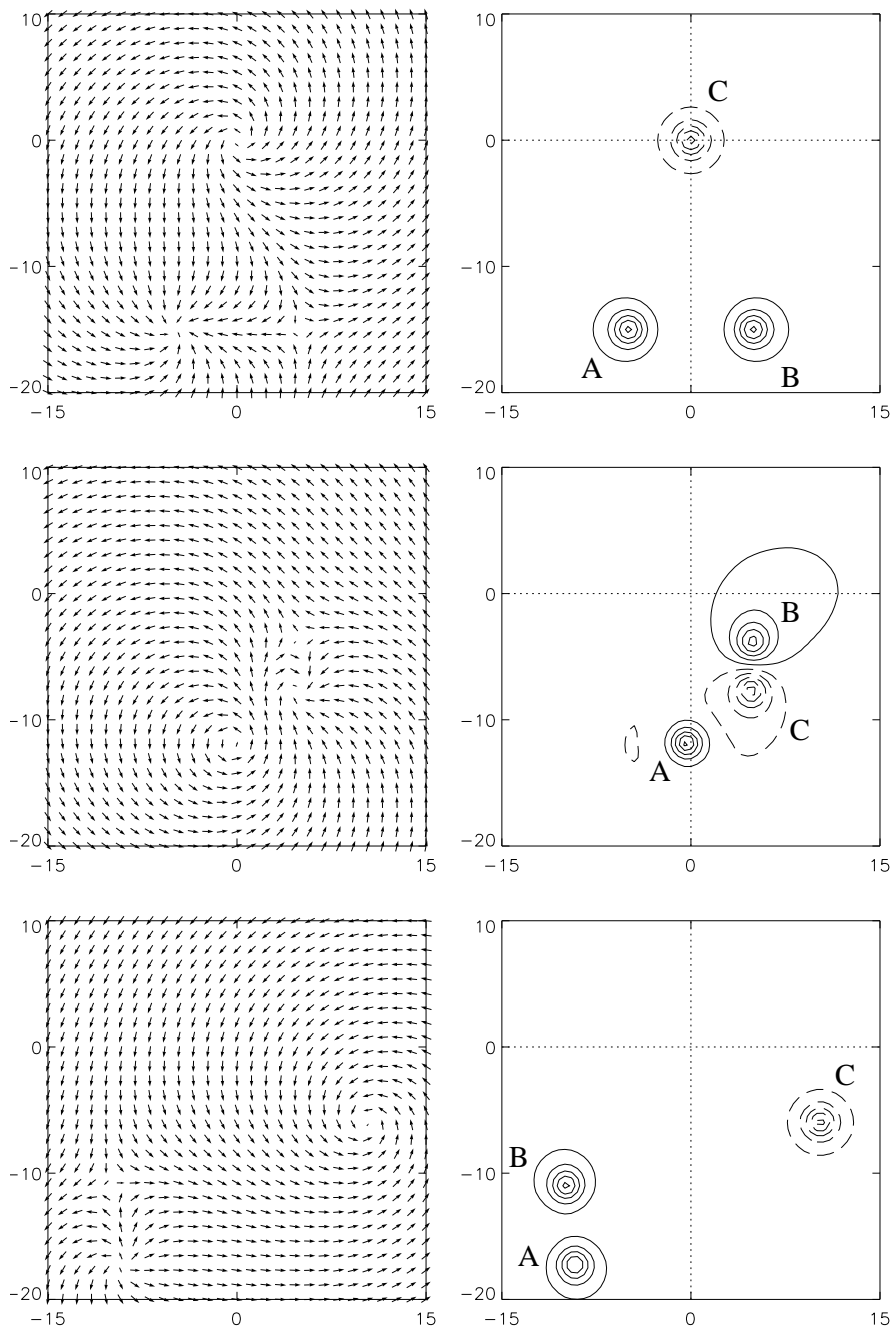


FIG. 8: Three snapshots for the collision of a VA pair in Kelvin motion (the AB pair), initially located at $(0, -15)$ and propagating with velocity $v = 0.1$, against a target vortex C initially located at the origin. During collision, antivortex B rotates around vortex C before rejoining its original partner A to form a new VA pair that scatters off at an angle in the third quadrant. The target vortex C is shifted to a new position in the fourth quadrant thanks to transmutation of VA pair momentum to vortex position.

systems, such as the three-vortex system considered here (a more detailed discussion will be given in a future publication).

The preceding numerical experiment was repeated for a Kelvin pair with relatively large velocity $v = 0.5$ for which the vortex and the antivortex are tightly bound at a relative distance $d = 2.6$ [17]. The process is again illustrated by three characteristic snapshots in Figure 9. While the initial stages of the process are similar to those encountered in the case of slow Kelvin motion (Figure 8) a substantial departure occurs when the pair now approaches the target vortex. In particular, as soon as antivortex $B = (-1, 1)$ begins to rotate around the target vortex $C = (1, -1)$ they collide and undergo a spectacular $\Delta\mathcal{N} = 1$ transition

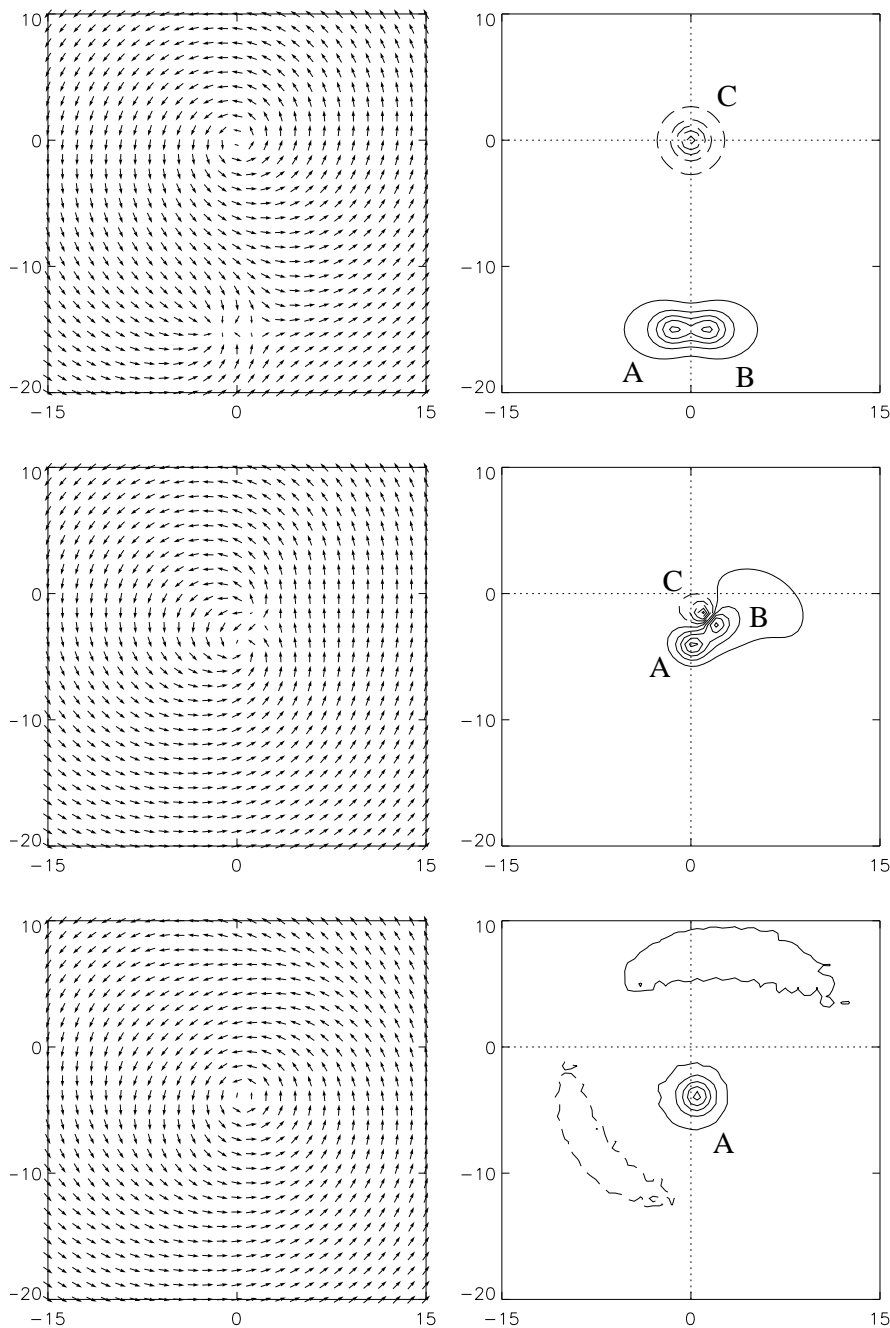


FIG. 9: Same as Fig. 8 but for a larger initial velocity $v = 0.5$ of the AB pair. During collision, antivortex B begins to rotate around vortex C but the rotating BC pair is eventually annihilated leaving behind vortex A (with polarity opposite to that of the target vortex C) and a burst of spin waves that propagate away from the scattering region.

(annihilation) leaving behind the $A=(1, 1)$ vortex which may be thought of as the target vortex $C=(1, -1)$ with polarity flipped from -1 to 1 (vortex core switching) and a burst of spin waves propagating away from the scattering region.

A detailed numerical investigation of the three-vortex process for Kelvin waves with velocities in the allowed range $0 < v < 1$ suggests the existence of the three characteristic regions separated by two critical velocities $v_1 = 0.3$ and $v_2 = 0.9$ (such that $0 < v_1 < v_0 < v_2 < 1$, with $v_0 = 0.78$ being the critical velocity discussed in Section III). For $0 < v < v_1$, the Kelvin pair undergoes nearly elastic scattering of the type depicted in Figure 8. For $v_1 < v < v_2$, the process leads to a topologically forbidden $\Delta\mathcal{N} = 1$

transition of the type illustrated in Figure 9. There is also some evidence that fast Kelvin waves with velocities in the narrow range $v_2 < v < 1$ undergo a nearly elastic scattering without inversion of the polarity of the target vortex.

VI. CONCLUSION

The VA pairs analyzed in this paper are special examples of solitary waves whose dynamics is closely related to their topological structure. For example, the VA pairs studied in Section III can undergo free translational motion because their topological charge vanishes ($\mathcal{N} = 0$). In contrast, a VA pair with nonvanishing \mathcal{N} performs rotational motion around a fixed guiding center and is thus spontaneously pinned within the ferromagnetic medium, as discussed in Section IV. Such a peculiar dynamical behavior would have been surprising had it not occurred previously in the case of interacting electric charges in the presence of a magnetic field.

It is then interesting to ascertain conditions under which a certain field theory would exhibit a similar link between topology and dynamics. A simple criterion was introduced in Ref. [22] and is briefly summarized as follows. We restrict attention to 2D Hamiltonian systems described in terms of Λ pairs of canonically conjugate variables (Π_i, Φ_i) with $i = 1, 2, \dots, \Lambda$. Then one may define the local vorticity

$$\gamma = \sum_{i=1}^{\Lambda} \epsilon_{\alpha\beta} \partial_{\alpha} \Pi_i \partial_{\beta} \Phi_i \quad (37)$$

which is a simple generalization of the first step of Eq. (9), the remaining two steps being special to the specific example considered in the present paper (ferromagnets). Now, in general, the total vorticity $\Gamma = \int \gamma dx dy$ is expected to vanish by a trivial partial integration using Eq. (37). On the other hand, a nonzero Γ would signal a special topological structure of the field theory under consideration and may lead to peculiar dynamics. The theory analyzed in the present paper is an example (with $\Lambda = 1$) which yields a nonzero Γ that may be identified with the Pontryagin index $\mathcal{N} = \Gamma/4\pi$. An example with $\Lambda = 2$ is provided by a 2D antiferromagnet where $\Gamma = 0$ except when an external field is present which may lead to $\Gamma \neq 0$ and an interesting link between topology and dynamics [22].

Implicit in the preceding general argument is the fact that a topological charge \mathcal{N} is conserved. Also taking into account that \mathcal{N} is quantized, one would expect that a topological ($\mathcal{N} \neq 0$) soliton cannot be annihilated in a continuous manner. Nevertheless, a quasi-continuous process was described in Ref. [18] and in the present paper according to which a rotating VA pair with $\mathcal{N} = 1$ may be reduced to a singular point and thereby be eliminated by lattice discreteness without encountering an energy barrier.

A mechanism for changing the topological number of a magnetic configuration makes it possible to obtain controlled switching between topologically distinct (and thus robust) magnetic states. This was achieved in the experiments of Refs. [13, 14]. The dynamics underlying both experiments involves a three-vortex process [15] initiated by the production of a topologically trivial VA pair in the vicinity of a preexisting vortex by an alternating magnetic field. It has been predicted that the same phenomenon would occur if one uses a rotating external field [31]. The resulting three-vortex system carries nonzero topological charge and is thus by itself a rotating object spontaneously pinned in the magnet. Also due to dissipation, a quasi-continuous process takes place that changes the topological number by one unit, leaving behind a burst of energy in the form of spin waves and a single vortex with polarity opposite to that of the original vortex.

Although our strictly 2D treatment provides a detailed scenario for the three-vortex process that leads to polarity switching, it does not account for the initial production of a topologically trivial VA pair. This is partly due to our approximation of a thin film with infinite extent. Implicit in this approximation is the assumption that the demagnetizing field amounts to a simple (additive) renormalization of easy-plane anisotropy. While this assumption appears to be firmly established for static magnetic states [19] we do not know of a corresponding mathematical derivation for dynamical processes of the type discussed here.

It is also important to visualize how the formation of a singular point discussed in the present strictly 2D context appears within a realistic magnetic element of finite extent. Numerical simulations [15] show that, in an element of finite thickness, a singular point is first created at one of the surfaces of the element. The VA pair then vanishes by formation and subsequent annihilation of a singular point at successive levels away from the surface. At the stage when a singular point has been formed and annihilated, say, near the top surface, while the VA pair is still present in the bulk of the element, a Bloch Point

(BP) is created in the element. This is a somewhat simplified realization of the BP studied in Ref. [32]. Needless to say, the BP created near the top surface is eventually annihilated when the VA pair exits the system through the lower surface. It is important to emphasize the unusual fact that during creation and annihilation of the BP the system does not have to overcome an energy barrier, unlike the case discussed in [33], essentially for the same reasons explained for the strictly 2D VA pairs studied in the main text.

Acknowledgments

N.P. is grateful for hospitality at the Max-Planck Institute for the Physics of Complex Systems (Dresden) where this work was completed.

APPENDIX A: ELECTRIC CHARGES IN A MAGNETIC FIELD

Most of the distinct features of the dynamics of VA pairs occur also in the dynamics of electric charges in the presence of a uniform magnetic field \mathbf{B} . Although we shall mainly be interested in 2D motion in a plane perpendicular to \mathbf{B} , it is convenient to keep for the moment 3D notation and write the equations of motion for two interacting charges e_1 and e_2 :

$$m \frac{d\mathbf{v}_1}{dt} = \mathbf{F}_1 + e_1(\mathbf{v}_1 \times \mathbf{B}), \quad m \frac{d\mathbf{v}_2}{dt} = \mathbf{F}_2 + e_2(\mathbf{v}_2 \times \mathbf{B}), \quad (\text{A1})$$

where

$$\mathbf{F}_1 = -\mathbf{F}_2 = -\frac{\mathbf{r}_1 - \mathbf{r}_2}{|\mathbf{r}_1 - \mathbf{r}_2|} V'(|\mathbf{r}_1 - \mathbf{r}_2|) \quad (\text{A2})$$

is the mutual force derived from a potential energy $V = V(|\mathbf{r}_1 - \mathbf{r}_2|)$ and V' denotes derivative with respect to the argument $|\mathbf{r}_1 - \mathbf{r}_2|$. The conserved energy functional is then given by

$$E = \frac{1}{2}m(v_1^2 + v_2^2) + V(|\mathbf{r}_1 - \mathbf{r}_2|), \quad (\text{A3})$$

which does not depend explicitly on the magnetic field, while the conserved linear momentum (impulse) is now given by

$$\mathbf{P} = m(\mathbf{v}_1 + \mathbf{v}_2) - (e_1\mathbf{r}_1 + e_2\mathbf{r}_2) \times \mathbf{B} \quad (\text{A4})$$

and differs from the usual mechanical definition by an important field dependent term. This (second) term actually indicates a rather profound influence of the magnetic field on the dynamics of electric charges. For instance, note that a shift of the origin of coordinates by a constant vector \mathbf{c} , thus $\mathbf{r}_1 \rightarrow \mathbf{r}_1 - \mathbf{c}$ and $\mathbf{r}_2 \rightarrow \mathbf{r}_2 - \mathbf{c}$, induces a nontrivial change on the impulse \mathbf{P} of Eq. (A4) given by

$$\mathbf{P} \rightarrow \mathbf{P} + (e_1 + e_2)(\mathbf{c} \times \mathbf{B}). \quad (\text{A5})$$

This unusual behavior is analogous to that of the impulse defined by Eq. (11) in the case of field configurations with nonvanishing total topological vorticity Γ or skyrmion number \mathcal{N} . Here we may abstract from Eq. (A5) the analog of the topological vorticity in the present problem:

$$\Gamma \sim (e_1 + e_2) B. \quad (\text{A6})$$

An electron-positron pair ($\Gamma = 0$) may undergo Kelvin motion, while two like charges ($\Gamma \neq 0$) perform rotational motion around a fixed guiding center, as determined by the explicit solutions constructed and briefly analyzed in the remainder of this appendix.

Consider first the case of an electron-positron pair ($e_1 = -e_2 = e$) for which a special 2D solution of Eqs. (A1) is given by

$$\begin{aligned} x_1 &= \frac{d}{2}, & y_1 &= vt, & z_1 &= 0, \\ x_2 &= -\frac{d}{2}, & y_2 &= vt, & z_2 &= 0, \end{aligned} \quad (\text{A7})$$

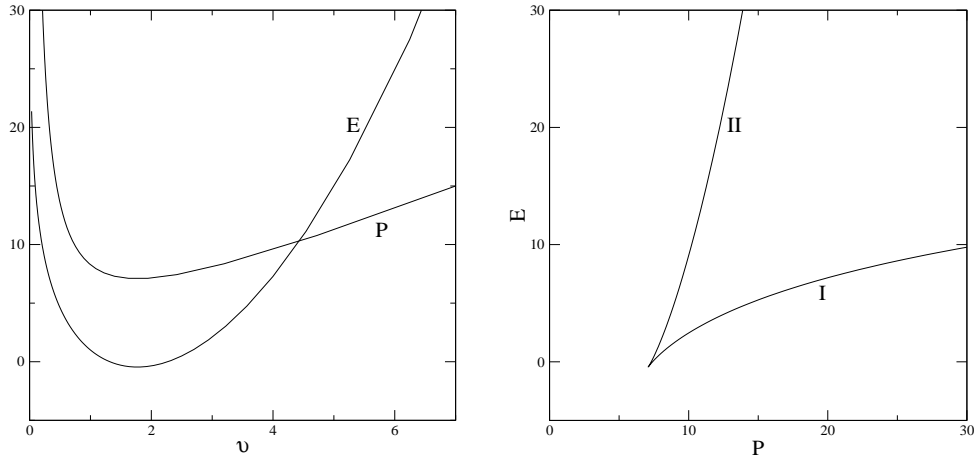


FIG. 10: Energy E and impulse P as functions of velocity v (left panel) and E vs P dispersion (right panel) for an electron-positron pair ($e_1 = -e_2$) in Kelvin motion.

where the electron and the positron are located at a constant relative distance d along the x axis and move in formation along the y axis with constant velocity

$$v = \frac{V'(d)}{eB}, \quad (\text{A8})$$

in close analogy with the Kelvin motion of the VA pair discussed in Section III. We further calculate energy E from Eq. (A3) and impulse $\mathbf{P} = (0, P, 0)$ from Eq. (A4) to find

$$\begin{aligned} E &= mv^2 + V(d) = m \left[\frac{V'(d)}{eB} \right]^2 + V(d) \\ P &= 2mv + eBd = 2m \frac{V'(d)}{eB} + eBd. \end{aligned} \quad (\text{A9})$$

Hence all relevant quantities are given in parametric form as functions of relative distance d once the potential energy $V = V(d)$ has been specified. But there are some generic properties of this solution that are practically independent of the choice of $V(d)$. We may take derivatives with respect to d of both sides of Eq. (A9) to find $E' = V'(1 + 2mV''/e^2B^2)$ and $P' = eB(1 + 2mV''/e^2B^2)$. An immediate consequence of these relations is the group-velocity relation $v = dE/dP$. We also note that both E and P may acquire an extremum at a common value of d (or v) determined from

$$1 + \frac{2mV''(d)}{e^2B^2} = 0. \quad (\text{A10})$$

This is actually the reason for the appearance of a cusp in the E vs P dispersion analogous to that encountered in the Kelvin motion of VA pairs, which now appears to be a generic feature of a wide class of physical systems.

For an explicit demonstration we make the special choice of potential energy

$$V = 2\pi \ln |\mathbf{r}_1 - \mathbf{r}_2| \quad (\text{A11})$$

in order to model the behavior of VA pairs at large relative distance [16, 34]. For a graphical illustration we also make the special choice of constants $m = 1$ and $eB = 2\pi$, as suggested by Eq. (A6), to write

$$v = \frac{1}{d}, \quad E = \frac{1}{d^2} + 2\pi \ln d, \quad P = \frac{2}{d} + 2\pi d \quad (\text{A12})$$

where we note that both E and P acquire a minimum at a distance $d = d_0 = 1/\sqrt{\pi}$ or velocity $v = v_0 = \sqrt{\pi}$. The dependence of E and P on the velocity v as well as the E vs P dispersion are shown in Fig. 10 and are found to be closely analogous to the results of Fig. 4 pertaining to Kelvin motion of VA pairs. In particular, for a widely separated pair (branch I) we find from Eq. (A12) that $P \sim 2\pi d$, $vP \sim 2\pi$, $v =$

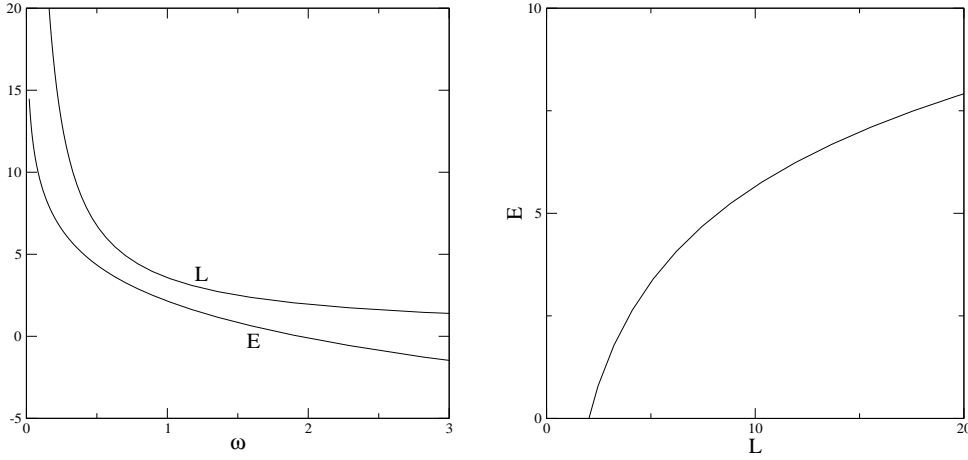


FIG. 11: Energy E and angular impulse L as functions of angular velocity ω (left panel) and E vs L dispersion (right panel) for a pair of like charges ($e_1 = e_2$) rotating around a fixed guiding center.

$1/d$, and $E = 2\pi \ln(P/P_0)$ with $P_0 = 2\pi$, in close analogy with the asymptotic results of Eqs. (22)–(24). The appearance of a cusp and consequently of branch II in the spectrum is also notable. But the details of branch II are different than those of Fig. 4 and Eq. (26). There is now no upper limit in the velocity v . In fact, all v, E and P in Eq. (A12) diverge in the limit of small d and $E \sim P^2/4$, which coincides with the dispersion $P^2/2M$ of a free particle with mass equal to the total mass of the pair ($M = 2m = 2$).

We have also carried out a stability analysis of the special Kelvin-like solution (A7) to find that the motion is marginally stable along branch I but becomes unstable along branch II. This conclusion is in agreement with a similar result obtained in Ref. [26] in the case of a vortex ring in a superfluid, as is further discussed in the concluding remarks of our Section III.

As a last example we consider the case of 2D motion of two like charges $e_1 = e_2 = e$. Then a special solution of Eq. (A1) is given by

$$x_1 = -x_2 = R \cos \omega t, \quad y_1 = -y_2 = R \sin \omega t, \quad z_1 = z_2 = 0 \quad (\text{A13})$$

which describes a pair rotating at constant radius $R = d/2$ and angular frequency $\omega = v/R$ where the velocity v is determined from the algebraic equation

$$\frac{mv^2}{R} + eBv - V'(d) = 0 \quad (\text{A14})$$

that expresses the exact balance of the centrifugal, the magnetic, and the mutual force. The conserved energy is still calculated from Eq. (A3) with $v_1^2 = v_2^2 = v^2$, but the conservation of the impulse \mathbf{P} of Eq. (A4) is simply equivalent to the statement that rotation takes place around a fixed guiding center. More relevant is now the conserved angular momentum (impulse) which is given by

$$L = m(x_1 \dot{y}_1 - y_1 \dot{x}_1) + \frac{e_1 B}{2}(x_1^2 + y_1^2) + m(x_2 \dot{y}_2 - y_2 \dot{x}_2) + \frac{e_2 B}{2}(x_2^2 + y_2^2), \quad (\text{A15})$$

where the overdot denotes time derivative. Again, the angular momentum differs from its standard mechanical expression by important field-dependent terms.

Now, for the specific choice of potential energy given by Eq. (A11), and constants $m = 1, e_1 = e_2 = e$ and $eB = 2\pi$, the algebraic equation (A14) yields

$$v = \pi \left(\sqrt{R^2 + \frac{1}{\pi}} - R \right), \quad R \equiv \frac{d}{2}, \quad (\text{A16})$$

while the angular velocity ω , the energy E , and the angular momentum L , read

$$\omega = \frac{v}{R}, \quad E = v^2 + 2\pi \ln(2R), \quad L = 2Rv + 2\pi R^2. \quad (\text{A17})$$

In view of Eq. (A16) all three quantities in (A17) are expressed in terms of a single parameter $R = d/2$. As a check of consistency one may verify the relation $\omega = dE/dL$ using Eqs. (A16–A17).

The dependence of E and L on angular velocity ω as well as the E vs L dispersion are shown in Fig. 11. Again there exists a close analogy with the results of Section IV on rotating VA pairs. In particular, for large diameter d , Eqs. (A17) yield $L \sim \frac{\pi}{2}d^2$, $\omega L \sim \pi$, $\omega \sim 2/d^2$, and $E = \pi \ln(L/L_0)$ with $L_0 = \pi/2$, which should be compared with the asymptotic results for VA pairs given in Eqs. (28)–(30). On the other hand, some quantitative differences arise at small d , where the angular momentum vanishes as expected ($L \sim \sqrt{\pi}d$) but the angular frequency diverges ($\omega \sim 2\sqrt{\pi}/d$). Furthermore, the energy E does not reach a finite value at $L = 0$ (as was the case for rotating VA pairs) but diverges logarithmically to minus infinity.

Finally, an analysis of mechanical stability [35] shows that circular motion of two like charges in a magnetic field is marginally stable for all values of d , in contrast to the Kelvin motion discussed earlier in this section which becomes unstable at small d . However, unlike Kelvin motion which proceeds with no acceleration, a rotating pair is expected to radiate when full electrodynamics is turned on. Surely, this is also a source of instability and may indicate a similar instability for the rotating VA pairs discussed in Section IV.

-
- [1] A. P. Malozemoff and J. C. Slonczewski, *Magnetic Domain Walls in Bubble Materials* (Academic Press, New York, 1979).
- [2] A. Hubert and R. Schäfer, *Magnetic domains* (Springer, Berlin, 1998).
- [3] D. L. Huber, *Phys. Rev. B* **26**, 3758 (1982).
- [4] F. Mertens and A. Bishop, “Dynamics of Vortices in Two-Dimensional Magnets” in P.L. Christiansen and M.P. Sorensen (eds.), “Nonlinear Science at the Dawn of the 21st Century”, Springer, 1999.
- [5] A. A. Thiele, *J. Appl. Phys.* **45**, 377 (1974).
- [6] G. K. Batchelor, *An Introduction to Fluid Dynamics* (Cambridge University Press, Cambridge, 1967).
- [7] P. G. Saffman, *Vortex Dynamics* (Cambridge University Press, Cambridge, 1992).
- [8] R. Donnelly, *Quantized vortices in Helium II* (Cambridge University Press, Cambridge, 1991).
- [9] J. Raabe, R. Pulwey, R. Sattler, T. Schweiböck, J. Zweck, and D. Weiss, *J. Appl. Phys.* **88**, 4437 (2000).
- [10] K. Shigeto, T. Okuno, K. Mibu, T. Shinjo, and T. Ono, *Appl. Phys. Lett.* **80**, 4190 (2002).
- [11] F. J. Castano, C. A. Ross, C. Frandsen, A. Eilez, D. Gil, H. I. Smith, M. Redjidal, and F. B. Humphrey, *Phys. Rev. B* **67**, 184425 (2003).
- [12] A. Neudert, J. McCord, R. Schäfer, and L. Schultz, *J. Appl. Phys.* **97**, 10E701 (2005).
- [13] B. V. Waeyenberge, A. Puzic, H. Stoll, K. W. Chou, T. Tylizszczak, R. Hertel, M. Fähnle, H. Brückl, K. Rott, G. Reiss, I. Neudecker, D. Weiss, C. H. Back, and G. Schütz, *Nature(London)* **444**, 461 (2006).
- [14] K. Yamada, S. Kasai, Y. Nakatani, K. Kobayashi, H. Kohno, A. Thiaville, and T. Ono, *Nature Materials* **6**, 269 (2007).
- [15] R. Hertel, S. Gliga, M. Fähnle, and C. M. Schneider, *Phys. Rev. Lett.* **98**, 117201 (2007).
- [16] V. L. Pokrovskii and G. V. Uimin, *JETP Lett.* **41**, 128 (1985).
- [17] N. Papanicolaou and P. N. Spathis, *Nonlinearity* **12**, 285 (1999).
- [18] S. Komineas, *Phys. Rev. Lett.* **99**, 117202 (2007).
- [19] G. Gioia and R. D. James, *Proc. R. Soc. Lond. A* **453**, 213 (1997).
- [20] N. Papanicolaou and T. N. Tomaras, *Nucl. Phys. B* **360**, 425 (1991).
- [21] S. Komineas and N. Papanicolaou, *Physica D* **99**, 81 (1996).
- [22] S. Komineas and N. Papanicolaou, *Nonlinearity* **11**, 265 (1998).
- [23] A. R. Völker, G. M. Wysin, F. G. Mertens, A. R. Bishop, and H. J. Schnitzer, *Phys. Rev. B* **50**, 12711 (1994).
- [24] K. S. Buchanan, P. E. Roy, M. Grimsditch, F. Y. Fradin, K. Yu. Guslienko, S. D. Bader, and V. Novosad, *Nature Materials* **1**, 172 (2005).
- [25] C. A. Jones and P. H. Roberts, *J. Phys. A: Math. Gen.* **15**, 2599 (1982).
- [26] C. A. Jones, S. J. Putterman, and P. H. Roberts, *J. Phys. A: Math. Gen.* **19**, 2991 (1986).
- [27] A. A. Belavin and A. M. Polyakov, *JETP Lett.* **22**, 245 (1985).
- [28] R. Hertel and C. M. Schneider, *Phys. Rev. Lett.* **97**, 177202 (2006).
- [29] O. A. Tretiakov and O. Tchernyshyov, *Phys. Rev. B* **75**, 012408 (2007).
- [30] K. Kuepper, M. Buess, J. Raabe, C. Quitmann, and J. Fassbender, *Phys. Rev. Lett.* **99**, 167202 (2007).
- [31] V. P. Kravchuk, D. D. Sheka, Y. Gaididei, and F. G. Mertens, *J. Appl. Phys.* **102**, 043908 (2007).
- [32] W. Döring, *J. Appl. Phys.* **39**, 1006 (1968).
- [33] J. C. Slonczewski, *AIP Conf. Proc.* **24**, 613 (1975).
- [34] A. Kovalev, S. Komineas, and F. G. Mertens, *Eur. Phys. J. B* **65**, 89 (2002).
- [35] T. E. Dialynas and E. G. Floratos, *Phys. Lett. A* **228**, 363 (1997).